

# 3D Simulation on Multiple Off-takes Branching Channel with Separation Zones

Siti Aimi Asyarah Zakaria<sup>1,a\*</sup>, Mohd Ridza Mohd Haniffah<sup>2,b</sup>, Taufiq Khairi Ahmad Khairuddin<sup>3,c</sup>, Iskandar Shah Mohd Zawawi<sup>4,d</sup>

<sup>1,2</sup>Department of Water and Environmental Engineering, Faculty of Civil Engineering, Universiti Teknologi Malaysia, Johor Bahru, 81310, Johor, MALAYSIA.

<sup>3</sup>Centre for Industrial and Applied Mathematics (CIAM), Universiti Teknologi Malaysia, Johor Bahru, 81310, Johor, MALAYSIA.

<sup>4</sup>School of Mathematical Sciences, College of Computing, Informatics and Mathematics, Universiti Teknologi MARA, Shah Alam, 40450, Selangor, MALAYSIA.

\*Corresponding Author

Email: <sup>a</sup>saasyarah2@graduate.utm.my, <sup>b</sup>mridza@utm.my, <sup>c</sup>taufiq@utm.my, <sup>d</sup>iskandarshah@uitm.edu.my

Received 05 March 2025;

Accepted 08 June 2025;

Available online 28 June 2025

**Abstract:** River diversions for flood mitigation purposes are scientifically considered as river bifurcation. The flow mechanism and dynamics of the bifurcated river need to be quantified during design phase of river diversion projects so that the diverted or branched river will serve its purpose when constructed. Computational modelling 3D Navier Stokes equation of FLOW-3D was employed to understand the behaviour of bifurcated river at varying off-take angles. Trapezoidal branching channel was setup with six off-take angles,  $\theta$ : 15°, 30°, 45°, 60°, 75° and 90° to investigate the relationship between the discharge ratio,  $Q_r$  and off-take angle,  $\theta$  in branching channels and also, its separation zone in the branch channel. The model was validated by previous laboratory experiment. Three different mesh size were used, Mesh 1 and Mesh 2 converged with 4.77% error, hence Mesh 1 was chosen for the simulations. The findings reveal a notable inverse correlation: as  $\theta$  increased,  $Q_r$  decreased. Additionally, the width of separation,  $S_w$  demonstrates variable behaviours with increasing  $\theta$ . Within the range of 15° to 45°, both  $S_w$  and  $Q_r$  exhibit an increase. However, for  $\theta$  between 60° and 90°,  $Q_r$  decreases, consequently leading to a decrease in  $Q_r$ . Furthermore, the study examines the length of separation,  $S_L$ . It is observed that as  $\theta$  increases from 15° to 45°,  $S_L$  decreases consistently. However, the results become less predictable as  $\theta$  approaches 90°. These findings contribute to a deeper understanding of flow separation dynamics in branching channels and can assist in the design of river diversion.

**Keywords:** river bifurcation, river diversion, branching channel, computational modelling, multiple off-takes

## 1. Introduction

Flow separation in a branching channel occurs when the flow splits into two or more rivers. This phenomenon is commonly observed in various engineering and natural system such as river and deltas. To understand the flow separation in branching channel is crucial as it's a complex phenomenon influenced by various factors such as geometry, flow conditions, turbulence, and boundary layer effects.

With regards to branching channel, there are studies of discharge ratio and off-take angle by Obasi & Oloke (2013) where multiple off-take angles at a convex shape was applied for water irrigation purpose in Amoli, Nigeria. The study found that the required discharged for water irrigation obtained when off-take angle 90° was used. Alomari et al. (2018b) constructed a physical model with diversion angles of 30°, 45°, 60°, 75° and 90° with different width ratio,  $B_r$  (29%, 38%, and 48%). The study focused on scouring process happened at the bifurcation junction. Malik (2018) investigated sediment transport in a bifurcation river with

angle diversion of 20°, 40° and 60° in an asymmetrical rectangular channel. From the experiment, it was found that the discharge ratio of branch to main channel increased as diversion angle increased and increased ratio of sediment discharge. In term of velocity, as the diversion angle increased, the average velocities at the branch channel decreased.

Mathematical modelling approached by Zawawi et al. (2019) considered two off-takes  $\theta_1$  and  $\theta_2$  for each the main and branched channel with angles of 15°, 30°, 45°, 60°, 75° and 90°. The derived equation calculated the flowrate in the main channel downstream with the upstream flowrate was known. Results obtained but further validation needed to be made because of a few assumptions such as water depth and velocities were constant across the channel, the effect of shear stress, vertical acceleration and friction force were neglected. Alomari et al. (2020) predicted sediment transport for diversion angles of 30°, 45°, 60°, 75° and 90° and three different width ratios,  $B_r$  i.e. 30%, 40% and 50%. The

experiment found that, instead of using 90° branching channel, the sediment discharge was management by changing the diversion angle to 30° and 60°.

In a branching channel, there are two common features caused river bifurcation. Fig. 1 shows the flow characteristics of 90° branching channel which includes the separation zone immediately near the entrance of the branch channel (Zone A), separation zone in the main channel parallel to the main flow (Zone B), a dividing streamline, and secondary circulation (secondary flow) developed in a plane normal to the main flow direction (Ibrahim et al., 2020). The recirculating flow in the branch channel depends on the discharge ratio and off-take angle but in laminar flow, the separation zone depends on the discharge ratio and Reynolds number,  $Re$  in the upstream main channel. Hayes et al. (1989) found in a 90° of branching, the recirculation zone in the branch is affected by increasing  $Re$ . At  $Re$  of 800, the first circulation appeared in the main channel, second separation zone in the branch and the appearance of third recirculation zone in the upper wall of the branch and fourth vortex at the right wall of the main branch. This is interesting because most of previous studies found the separation zone in the branch Zone A and a few for Zone B and most of them are for 90° of branching channel. The aim of this paper is to analyse the flow separation in a multiple off-take branching channels through computational fluid dynamics.

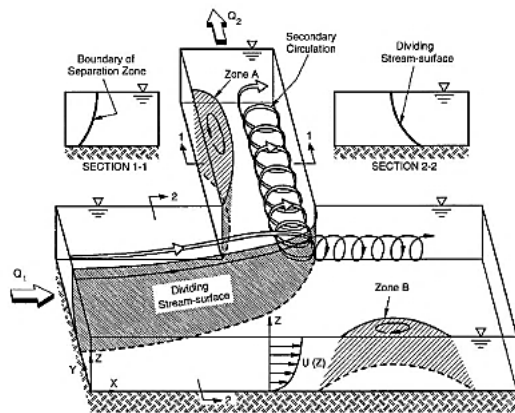


Fig. 1 - Separation zone in 90° off-take angle (Ibrahim et al., 2020)

## 2. Methodology

The study of the multiple off-take branching channel with a separation zone involved several key steps. First, the simulation was set up by defining the meshing, boundary conditions, initial boundaries, and selecting an appropriate turbulence model. Model validation was then performed by comparing the simulation results with experimental or theoretical benchmarks to ensure accuracy. A convergence study was conducted to assess the numerical stability and reliability of the simulations. The effect of vertical confinement on flow dynamics was also analyzed to capture its influence on the separation zone. These steps were designed to systematically investigate the flow behavior within the branching channel under varying conditions.

### 2.1 Simulation Setting Up

This study consists of simulation of multiple off-take branching channel using 3D simulation through FLOW-3D software. Fig. 2 shows the layout of the bifurcated channel. A trapezoidal cross-section channel with bottom width of 2.86 m

was used and side slope was 60°. The discharge was flowing from the left (upstream) and diverted into both the downstream and branch channels. The off-take angles,  $\theta$  considered for the bifurcated channel were 15°, 30°, 45°, 60°, 75° and 90°. The upstream discharge,  $Q_u$  was 10 m<sup>3</sup>/s. The discharge ratio is the ratio of flowrate in the downstream,  $Q_d$  to the flowrate in the upstream channel,  $Q_u$ . Then, the vertical confinement and flow separation in multiple off-take branching channels were observed.

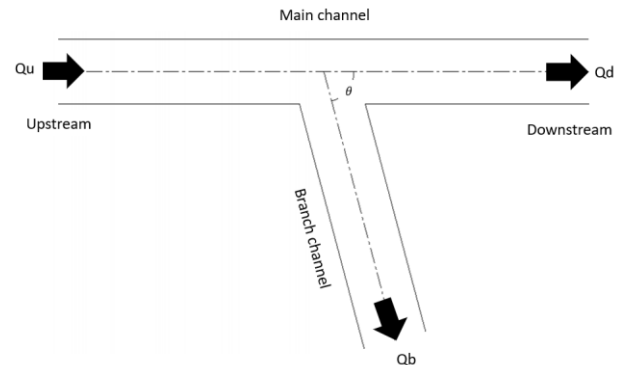


Fig. 2 - Layout of bifurcated channel

### 2.2 Physics Option in FLOW3D

In this simulation, two physics options were activated, gravitational acceleration and turbulence model. The gravitational acceleration in the vertical,  $z$  direction was set to -9.81 m/s<sup>2</sup>. As for the turbulence model, the RNG turbulence model was applied. The option of wall shear boundary conditions was automatically set to no slip condition when viscous flow was selected. The fluid properties as water 20°C was applied with density of 1000 kg/m<sup>3</sup> and viscosity of 0.001 kg/m/s.

### 2.3 Initial and Boundary Conditions

The initial and boundary conditions are unique to the problem. The initial condition was determined by the actual flow data, which includes the water elevation and hydrostatic pressure. To lessen the amount of water splashing and immediate change of velocity, the discharge at the upstream boundary was gradually increased from zero to the required discharge, hence increasing the stability of the simulation and shortening the time to reach its steady state.

Fig. 3 shows the selected boundary condition for the simulation. The main channel upstream was set to volumetric flowrate,  $Q$  and the outlet downstream of the main channel, Outlet 1 and the outlet of the downstream branch channel, Outlet 2 was set to outflow, O boundary condition. The boundary at the top of the channel was set to pressure, P boundary condition. While, the boundary at the bottom remained as symmetry, S boundary condition, followed the default condition.

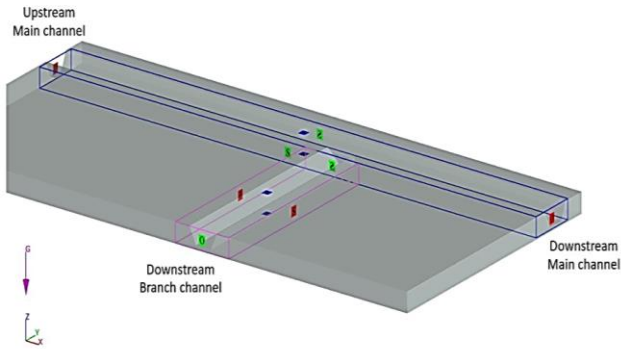


Fig. 3 - Selected boundary conditions

## 2.4 Model Validation

The simulation setup was validated using laboratory experiment data from Sayed (2019). The validation process involved comparing the effect of varying upstream discharge on the discharge ratio observed in simulation with the experimental results. This comparison ensured that the simulation accurately replicated the physical behavior of the flow in the branching channel and its reliability for further analysis.

The geometric setting up of 90° branching channel consists of 8.0 m of main channel length and 3.0 m branch channel. Both channels had uniform width and depth of 0.2 m. The downstream ends of main and branch were free from any hydraulics structure such as weir. The simulation was conducted using five different upstream discharges: 1.19, 1.78, 2.47, 3.37, and 4.00. The corresponding measured Froude numbers ranged from 0.4 to 0.76, capturing a range of subcritical flow conditions. Based on these upstream discharges, the discharge ratio for each case was calculated. The results presented in Fig. 4.

From the result, it shows that as the  $Q_u$  increased, the discharged ratio,  $Q_r$ , decreased. The results of FLOW-3D simulation and experimental data differ in values but good agreement in term of overall trend. This validates the simulation is able to recreate the 90° off-take branching channel flow, given the complexity at the junction with regards to the change in flow momentum with respect to the upstream discharge.

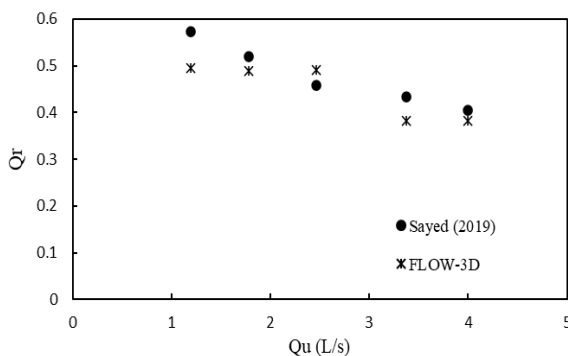


Fig. 4 - Validation of simulation and experiment results

## 2.5 Mesh Convergence Study

In present study, three mesh grid sizes were used, namely Mesh 1, Mesh 2 and Mesh 3. Mesh 1 is  $0.2 \times 0.2 \times 0.2$  m, Mesh 2 is  $0.1 \times 0.1 \times 0.1$  m, and Mesh 3 is  $0.08 \times 0.08 \times 0.08$  m. The aspect ratio for all mesh grid size is 1:1:1 (x: y: z). The

downstream velocity,  $V_d$  was used as the parameter for the convergence study for all off-take angles with upstream discharge of  $10 \text{ m}^3/\text{s}$ , and the results are shown in Table 1.

Table 1 - Percentage error for three meshes

$\theta$	$V_d$ (m/s)			% Error Mesh 1 & Mesh 2	% Error Mesh 1 & Mesh 3
	Mesh 1	Mesh 2	Mesh 3		
15°	1.36	1.39	1.40	2.06	3.00
30°	1.39	1.47	1.48	5.71	5.99
45°	1.36	1.30	1.42	4.07	4.68
60°	1.52	1.50	1.50	1.39	1.04
75°	1.32	1.49	1.55	13.10	17.30
90°	1.20	1.23	1.29	2.30	7.47
Average Error (%)				4.77	6.58

For the mesh selection, the average percentage error for all off-take angle is considered. From the results, Mesh 1 and Mesh 2 are already converged with an average percentage error of 4.77%. Since the difference between Mesh 1 and Mesh 2 is acceptable, Mesh 1 was chosen as the mesh size to simulate the flow through the branch channel for multiple off-take angles with equal width as the simulation was already converged with the courser mesh size, thus it shortens the simulation time.

## 2.6 Flow Field in Trapezoidal Channel

To identify the separation zone, the variation of the flow fields in the vertical direction must be known so that a layer of the fluid can be chosen to represent the results. However, due to the complexity of the geometric and hydraulic properties of the trapezoidal section, the fluid flow shown by the velocity magnitude with vectors for five vertical directions:  $z_1 = 0.48$  m,  $z_2 = 0.86$  m,  $z_3 = 1.15$  m,  $z_4 = 1.44$  m, and  $z_5 = 1.72$  m from the origin for  $Q_u$  was  $10 \text{ m}^3/\text{s}$  were selected.

## 3. Result and Discussion

### 3.1 Vertical Confinement

The method of vertical confinement of the trapezoidal channel was performed. Fig. 5 shows the velocity magnitude with vectors of the flow for upstream flowrate,  $Q_u = 10 \text{ m}^3/\text{s}$ . Vertical confinement for fives slices were investigated,  $z = 0.48$  m,  $0.86$  m,  $1.15$  m,  $1.44$  m and  $1.72$  m.

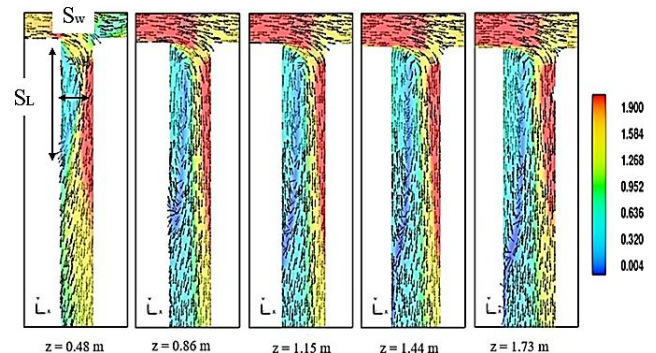


Fig. 5 - Velocity magnitudes (m/s) with vector each slice

The separation length,  $S_L$  near the branch channel's bed surface was the smallest and increased with increasing depth. But, the separation width,  $S_w$  was almost identical to each other. Furthermore, it can be found that, the velocity near the

bed surface,  $z = 0.48$  m was lower than velocity near the surface,  $z = 1.72$  m.

From the results, the flow field was homogeneous as the velocity field pattern through the water depth is almost identical. Hence, for the case of trapezoidal channel, the surface slice of plane was applied for the separation zone analysis as it has the highest and most significant velocity and separation zone.

### 3.2 Discharge Ratio

Fig. 6 shows the effect of off-take angles of  $15^\circ$ ,  $30^\circ$ ,  $45^\circ$ ,  $60^\circ$ ,  $75^\circ$  and  $90^\circ$  on the discharge ratio,  $Q_r = Q_d/Q_u$ . From the results, the  $Q_r$  increased slightly as  $\theta$  increased from  $15^\circ$  to  $30^\circ$ , then gradually decreased up to  $75^\circ$  of off-take before dropping significantly at  $90^\circ$ . In general,  $Q_r$  decreased as the  $\theta$  increased. As the  $\theta$  increased from  $15^\circ$  to  $90^\circ$ ,  $Q_r$  decreased by 26.6%. To understand the underlying physics for the relationship between  $Q_r$  and  $\theta$ , details of velocity and separation zone are discussed in the next section.

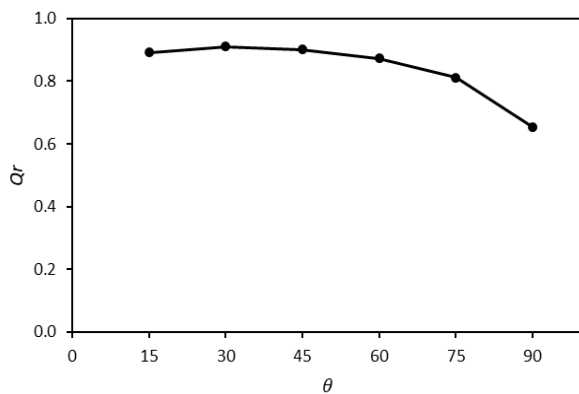


Fig. 6 - Relationship between  $Q_r$  and  $\theta$

### 3.3 Separation Zones

The separation zone for multiple off-take angles of branching channel is presented through the streamlines as shown in Fig. 7 for the upstream discharge  $10 \text{ m}^3/\text{s}$ . The streamlines in the figures can help to discover the size and location of the separation zone. The separation zone occurred at the entrance of the branch channel regardless of the off-take angles and upstream discharges. In addition, Fig. 7 (f) show a second separation zone at the main channel of off-take angle of  $90^\circ$ .

The velocity distribution of the separation zone in the bifurcation channel for all off-take angles are given in Fig. 8. The velocity distribution supports the results from the streamlines for each off-take angles. the separation zone occurred in the branch channel presented in the low velocity area. Naturally, the flow separation occurs due to the occurrence of adverse pressure gradient in the channel due to a sudden change in the flow direction. The adverse pressure gradient results in velocity against the main direction and will circulate.

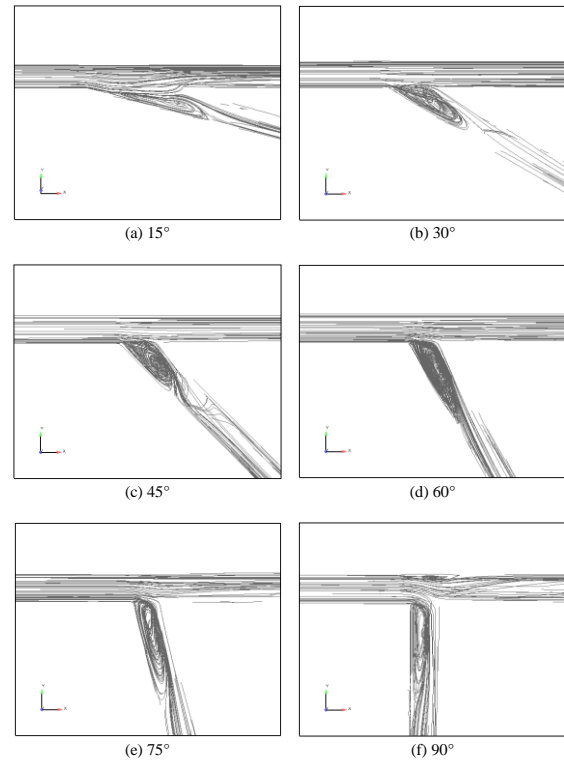


Fig. 7 - Streamlines of separation zones for various  $\theta$

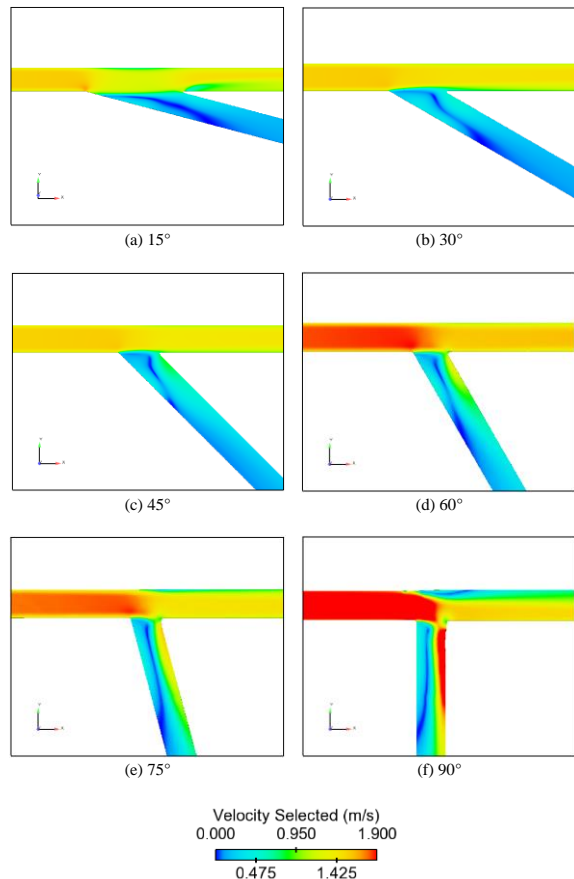


Fig. 8 - Velocity distribution of separation zones for various  $\theta$

There are also high upstream velocities at off-take angle of 90°. Most probably at this angle, the flow is fully developed i.e. the flow is steady from the upstream to both downstream and branched channels producing a less chaotic flow over time and hence a smooth flow into the branch. For other angles, maybe there is no steady flow over time due to the geometry of the angles. Further analysis can be done as recommendation for next research. Also, work done by Maurya et al. (2021) at a constant  $R_e$  and off-take angle, the circulation zone in the main and branch channels appeared when off-take angles were 30° and 90° due to centrifugal forced experienced by the fluid.

### 3.4 Relationship between Discharge Ratio and Separation Zones

Fig. 9 shows the effect of increasing off-take angle,  $\theta$  to the separation width,  $S_w$  for  $Q_u = 10 \text{ m}^3/\text{s}$ . As  $\theta$  increased from 15° to 45°, the  $S_w$  increased. But, as the  $\theta$  increased from 60° to 90°, the  $S_w$  decreased. Referring to Fig. 4, a relationship between  $\theta$ , discharge ratio and  $S_w$  were found, as the  $\theta$  increased from 15° to 45°,  $S_w$  and  $Q_r$  increased, while the  $\theta$  increased from 60° to 90°,  $S_w$  decreased.

While Fig. 10 shows the length of separation,  $S_L$ . The general trend shows that the  $S_L$  decreased as the  $\theta$  increased. From the results, as the  $\theta$  increased from 15° to 45°, the  $S_L$  decreased but when  $\theta$  increased to 90°, the results were not consistent. But the smallest  $S_w$  and  $S_L$  were found at 90° off-take angle.

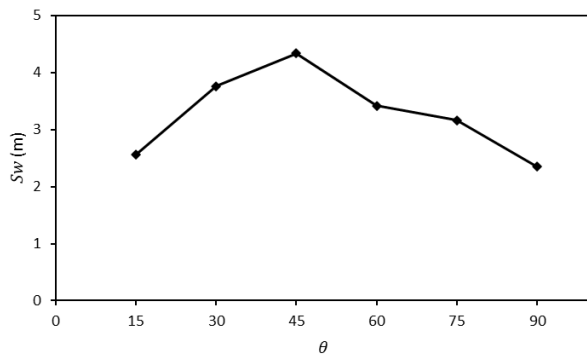


Fig. 9 - Relationship between  $\theta$  and  $S_w$

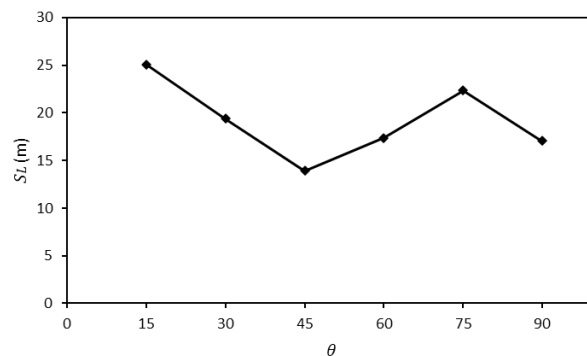


Fig. 10 - Relationship between  $\theta$  and  $S_L$

### 4. Conclusion

The aim of this paper is to analyze the flow mechanism for different off-take angles with separation zones. Overall  $S_w$  has greater impact on  $Q_r$  than  $S_L$ , with the off-take angle

playing a critical role in influencing  $S_w$  and discharge behaviour. A decrease in separation width increases the effective flow of the branch channel, enhancing flow into the branch and reducing downstream flow. As the off-take angle increase, the hydraulic resistance in the branch channel rises due to a sharper diversion, resulting reduction in the discharge ratio. The width of separation,  $S_w$  grows for smaller angles (15° to 45°) because the flow diversion less abrupt, allowing for wider separation zone and greater discharge into the branch, but at larger angle (60° and 90°), the flow separation become more pronounced, narrowing  $S_w$  and further reducing  $Q_r$ . The behaviour of the length of separation,  $S_L$  decreasing up to 45° represent the smoother flow transition at moderate angles. Beyond 45°, the inconsistent results likely arise from turbulent and secondary pattern that become dominant, resulting inconsistent results. The greater impact of  $S_w$  compared to  $S_L$  on  $Q_r$  highlights the importance of the effective width of the branch channel, enhancing flow into the branch. From these findings, it shows that the flow distribution in branching channel is highly sensitive to change of geometric and size of the separation zone.

### 5. Online License Transfer

All authors are required to complete the Procedia exclusive license transfer agreement before the article can be published, which they can do online. This transfer agreement enables Elsevier to protect the copyrighted material for the authors, but does not relinquish the authors' proprietary rights. The copyright transfer covers the exclusive rights to reproduce and distribute the article, including reprints, photographic reproductions, microfilm or any other reproductions of similar nature and translations. Authors are responsible for obtaining from the copyright holder, the permission to reproduce any figures for which copyright exists.

### Acknowledgement

This research work was funded under Collaborative Research Grant, UTM of reference Q.J130000.2451.08G89. This research is in collaboration with Universiti Teknologi MARA, under general collaboration involving University of Nottingham Malaysia, UNITEN and Universiti Teknologi Petronas.

### References

- [1] Alomari, N. K., Yusuf, B., Mohammad, T. A. & Ghazali, A. H. (2020). Influence of diversion angle on water and sediment flow into diversion channel. *International Journal of Sediment Research*, 35(6), 600–608. <https://doi.org/10.1016/j.ijsrc.2020.06.006>
- [2] Alomari, N. K., Yusuf, B., Mohammad, T. A., & Ghazali, A. H. (2018). Experimental investigation of scour at a channel junctions of different diversion angles and bed width ratios. *Catena*, 166, 10-20.
- [3] Hayes, R. E., Nandakumar, K., & Nasr-El-Din, H. (1989). Steady laminar flow in a 90 degree planar branch. *Computers & Fluids*, 17(4), 537-553.
- [4] Ibrahim, I., Ibrahim, S. L., & Khan, S. (2020, February). Flow structures in dividing open channels: a review. In *IOP Conference Series: Earth and*

Environmental Science (Vol. 437, No. 1, p. 012008).  
IOP Publishing.

- [5] Malik, L. (2018). Experimental study of flow and sediment distribution at river offtake.
- [6] Maurya, A., Tiwari, N., & Chhabra, R. P. (2021). Forced convective flow of Bingham plastic fluids in a branching channel with the effect of T-channel branching angle. *Journal of Fluids Engineering*, 143(5), 051201.
- [7] Obasi, N., & Oloke, D. Flow Distribution Design Charts for Bifurcation at Convex Channel Curvature.
- [8] Zawawi, I. S. M., Abdullah, N. L., Aris, H., Jaafar, B. A., Norwaza, N. A. H., & Yunus, M. H. F. M. (2019). Mathematical Modeling for Flood Mitigation: Effect of bifurcation Angles in River Flowrates. *Civil Engineering and Architecture*, 7(6A), 50-57.
- [9] Sayed, T. (2019). An experimental study of branching flow in open channels. *Limnological Review*, 19(2), 93–101. <https://doi.org/10.2478/limre-2019-0008>